The Cell Surface Membrane Proteins Cdo and Boc Are Components and Targets of the Hedgehog Signaling Pathway and Feedback Network in Mice

Toyoaki Tenzen,[1] Benjamin L. Allen,[1] Francesca Cole,[2]
Jong-Sun Kang,[2] Robert S. Krauss,[2]
and Andrew P. McMahon[1,*]
[1] Department of Molecular and Cellular Biology
Harvard University
16 Divinity Avenue
Cambridge, Massachusetts 02138
[2] Brookdale Department of Molecular, Cell,
   and Developmental Biology
Box 1020
Mount Sinai School of Medicine
One Gustave L. Levy Place
New York, New York 10029

Summary

Cdo and *Boc* encode cell surface Ig/fibronectin super-family members linked to muscle differentiation. Data here indicate they are also targets and signaling components of the Sonic hedgehog (Shh) pathway. Although *Cdo* and *Boc* are generally negatively regulated by Hedgehog (HH) signaling, in the neural tube *Cdo* is expressed within the Shh-dependent floor plate while *Boc* expression lies within the dorsal limit of Shh signaling. Loss of Cdo results in a Shh dosage-dependent reduction of the floor plate. In contrast, ectopic expression of Boc or Cdo results in a Shh-dependent, cell autonomous promotion of ventral cell fates and a non-cell-autonomous ventral expansion of dorsal cell identities consistent with Shh sequestration. Cdo and Boc bind Shh through a high-affinity interaction with a specific fibronectin repeat that is essential for activity. We propose a model where Cdo and Boc enhance Shh signaling within its target field.

Introduction

Hedgehog (HH) signals regulate the specification of complex patterns within embryonic fields as diverse as imaginal discs in *Drosophila* larvae and the neural tube and limb of vertebrate embryos (McMahon et al., 2003). In the neural tube, the induction of all ventral cell identities requires direct Sonic hedgehog (Shh) signaling; the actual cell fate choice is determined by the concentration of Shh ligand (reviewed in Briscoe and Ericson, 2001; Jessell, 2000). Shh is initially released from the midline notochord underlying the ventral neural plate/tube and later from the floor plate. The floor plate, a population of ventral midline support cells within the neural tube, is itself a target of Shh signaling that requires the highest levels of ligand for its induction (Ericson et al., 1997). Shh from these sources forms a gradient that extends over the ventral half of the neural tube (Gritli-Linde et al., 2001).

In these patterning processes, feedback mechanisms acting at the level of ligand binding play a critical role in determining both the number and full range of ventral cell types (reviewed in Ingham and McMahon, 2001). *Patched-1* (*Ptch1*) encodes the vertebrate HH receptor while *Hedgehog-interacting protein-1* (*Hhip1*) encodes an unrelated membrane-associated protein that similarly binds all mammalian HH ligands. *Ptch1* and *Hhip1* are upregulated in response to HH signaling; their feedback functions serve to modify the range of signaling and regional response of target cells (Chuang and McMahon, 1999; Jeong and McMahon, 2005). A third HH binding factor, Growth arrest-specific-1 (Gas1), is thought to inhibit Shh signaling; *Gas1* is itself repressed in response to HH signaling (Lee et al., 2001). Here we present evidence that *Cdo* and *Boc*, which encode cell surface bound members of the Ig/fibronectin domain superfamily, are novel feedback components that act in a different manner, to enhance Shh signaling within subregions of Shh's neural target field.

Results and Discussion

Cdo and Boc Are Targets of Shh Signaling that Cell Autonomously Enhance Shh Signaling

To attempt to identify novel, general feedback components, we compared transcriptional profiles (data not shown) from early, somite-stage mouse embryos, where HH signaling is either normal (wild-type embryos), absent (*Smoothened* [*Smo*] mutant embryos [Zhang et al., 2001]), or enhanced (*Ptch1* mutant embryos [Goodrich et al., 1997]), with profiles generated from microdissected tissues from later stage embryos where *Shh* signaling is lost (head and limb fractions from E10.5 *Shh* mutant embryos [St-Jacques et al., 1998]). Among those genes encoding cell surface or secreted proteins downregulated in response to Shh (enhanced expression in *Smo* and *Shh* mutants and repressed in *Ptch1* mutants), we identified *Gas1*, as expected, and two genes that encode related members of an Ig/fibronectin repeat-containing superfamily of cell surface, membrane-spanning proteins, *Cdo* (sometimes *Cdon* [Kang et al., 1997]) and *Boc* (Kang et al., 2002).

Cdo and Boc represent a subfamily within the Ig superfamily, consisting of an ectodomain comprised of four (Boc) or five (Cdo) Ig repeats, followed by three fibronectin type III (FNIII) repeats and a long, divergent intracellular domain (Kang et al., 1997, 2002). Interestingly, *Cdo* mutant mice exhibit a microform holoprosencephaly, wherein midline facial structures are absent, a phenotype reminiscent of a partial loss of Shh signaling (Cole and Krauss, 2003; Cooper et al., 1998; Tian et al., 2005). A further link to the HH pathway comes from an siRNA screen in *Drosophila* that lists a *Boc/Cdo* relative, CG9211, as a putative effector of HH signaling (Lum et al., 2003).

Cdo and *Boc* expression were examined in the developing mouse and chick embryo. In both, *Cdo* and *Boc* expression are excluded from most HH-signaling domains, consistent with negative regulation by HH signaling (Figure 1 and Figure S1 [see the Supplemental Data available with this article online], data not shown, and Mulieri et al. [2000, 2002]). In the neural tube and somites,
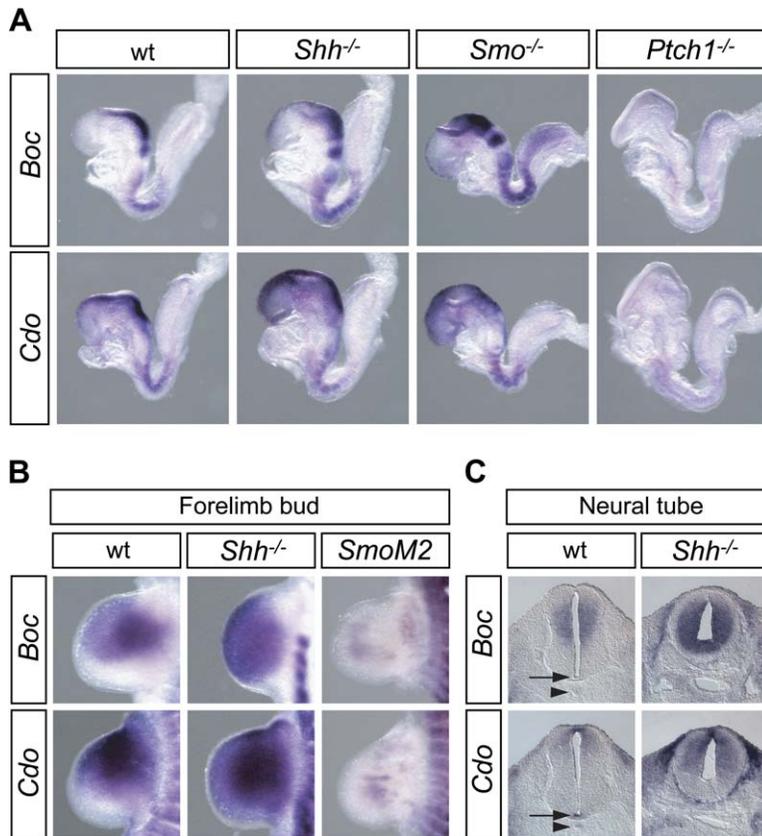
*Correspondence: mcmahon@mcb.harvard.edu

Figure 1. *Boc* and *Cdo* Are Negatively Regulated by Hedgehog Signaling

In situ hybridization analysis of *Boc* and *Cdo* expression in the developing mouse embryo.
(A) E8.5 (8–10 somite stage) mouse embryos show enhanced or ectopic expression of *Cdo* and *Boc* in *Shh* and *Smo* mutants, and repression in *Ptch1* mutants. Anterior to left, lateral views.
(B) *Boc* and *Cdo* expression expand into the posterior mesenchyme of *Shh* mutant forelimb buds at E10.5, but are broadly repressed on activation of HH signaling following ectopic expression of *SmoM2* throughout the limb mesenchyme. Anterior at top, dorsal views.
(C) *Cdo* and *Boc* expression in the E10.5 neural tube at the forelimb level. Dorsal *Cdo* and *Boc* expression is upregulated and their expression domains expand ventrally in the *Shh* mutant neural tube. *Cdo* also shows expression in the floor plate (arrow) and notochord (arrowhead); the former is lost in *Shh* mutants (see also Figure S1). Dorsal at top.

both genes are expressed dorsally, whereas in the limb, mesenchymal expression is restricted to the anterior two-thirds. On removal of HH signaling in *Smo* and *Shh* mutants, *Cdo* and *Boc* expression is enhanced, expanding ventrally in the somites and neural tube and to the posterior margin of the limb (Figure 1). In contrast, normal expression is lost, or markedly downregulated, both when HH signaling is derepressed in *Ptch1* mutants (Figure 1A) or ectopically activated following expression of a constitutively active allele of *Smo* (*SmoM2*, Figure 1B) (Jeong et al., 2004). Thus, *Cdo* and *Boc* appear to be negative targets of HH regulation in multiple HH-responsive tissues.

Whereas this conclusion is generally true, the relationship between *Cdo* and *Boc* expression domains and HH signaling is more complex. *Cdo* is transiently expressed at low levels within the notochord, a midline structure that produces, responds to, and requires Shh signaling (Figure S1) (Chiang et al., 1996; Echelard et al., 1993). Further, *Cdo* is weakly expressed at the ventral-mid line of the neural tube coincident with Shh-mediated induction of the rostral brain and caudal floor plate (arrow in Figure 1C and Figure S1; and see the accompanying paper by Zhang et al. [2006] in this issue of *Developmental Cell*). Finally, regions of active Shh signaling (as judged by upregulation of the general transcriptional targets *Ptch1* and *Gli1*) overlap the ventral boundary of *Boc* expression in the neural tube, and posterior boundaries of *Boc* and *Cdo* expression in the limb mesenchyme (Figure S2) (Gritli-Linde et al., 2002, 2001). Thus, *Cdo* and *Boc* may play active roles within specific HH-signaling domains.

To address this possibility, we determined whether *Cdo* and *Shh* genetically interact. $Cdo^{-/-}$ mutants have a mild holoprosencephalic phenotype; midline structures are lost, and left and right nasal processes, while separate structures, are positioned closer to the midline (Figure 2A) (Cole and Krauss, 2003). Although $Shh^{-/-}$ embryos exhibit an extreme holoprosencephalic phenotype, $Shh^{+/-}$ embryos are comparable to wild-type (Chiang et al., 1996). When *Shh* gene dosage is lowered in a *Cdo* mutant background ($Shh^{+/-}; Cdo^{-/-}$), the *Cdo* phenotype is dramatically enhanced; the nasal processes fuse into a single, proboscis-like structure, a hallmark of Shh deficiency (Figure 2A) (Chiang et al., 1996; Mulieri et al., 2000). The observed genetic interaction suggests that Cdo may normally promote Shh signaling.

Given *Cdo* expression in the floor plate, a structure induced by high levels of Shh signaling (McMahon et al., 2003), we characterized ventral patterning in the neural tube of these mutants. During normal floor plate development there is a transitory period wherein ventro-medial progenitors are Nkx2.2+ and Foxa2+. At later stages, Foxa2 is restricted to the definitive floor plate and Nkx2.2 to ventro-lateral vp3 progenitors of the V3 class of spinal interneurons (for reviews, see Briscoe and Ericson, 2001; Jessell, 2000). At this stage, *Shh* is activated in the floor plate; activation requires the activity of Foxa2, which binds directly to *Shh cis*-regulatory transcriptional control regions (Jeong and Epstein, 2003). At E10.5, Foxa2+ and Nkx2.2+ cell populations are largely independent cell populations in the neural tube of both wild-type and $Shh^{+/-}$ embryos (Figure 2B and data not shown). However, in *Cdo* mutants, few midline cells are Foxa2+
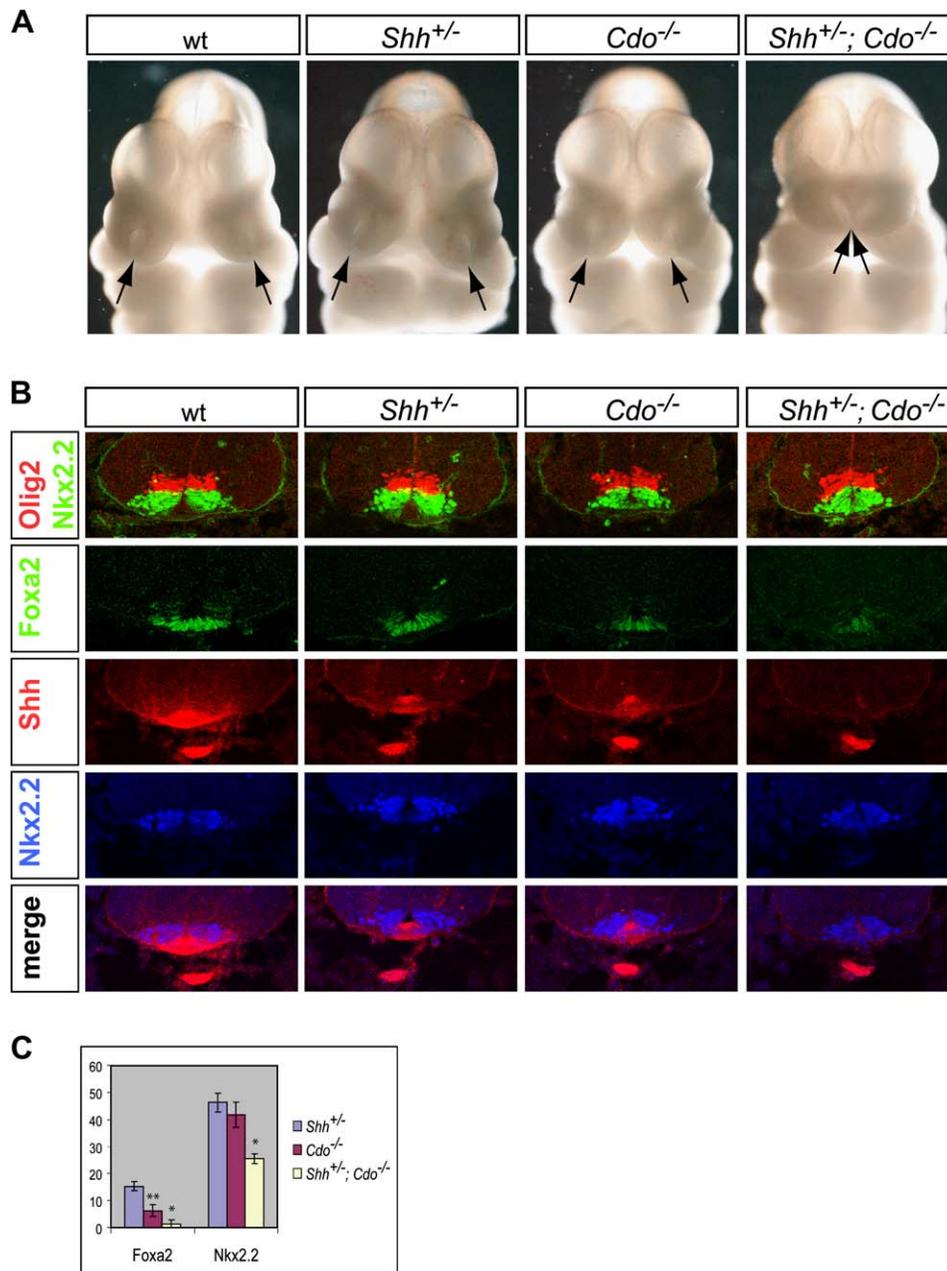
Figure 2. Genetic Interactions between *Cdo* and *Shh*

(A) Frontal views of facial development in E10.5 mouse embryos. The facial phenotype of *Cdo* mutants is greatly enhanced on lowering of *Shh* gene dosage. Paired olfactory pits (arrowed), normally separate structures, fuse at the midline in *Shh*^{+/−}*; Cdo*^{−/−} embryos.

(B) Immunostaining of the floor plate (Shh[+], Foxa2^{+}), vp3 (Nkx2.2[+]), and pMN (Olig2^{+}) progenitors in the E10.5 mouse neural tube at the forelimb level. Dorsal is at top.

(C) Quantitation of numbers of Foxa2^{+} and Nkx2.2^{+} cells above (n = 4). Bars represent standard deviation. ** indicates a significant difference in the number of Foxa2^{+} cells between *Shh*^{+/−} and *Cdo*^{−/−} embryos (p = 0.0007), while * indicates differences in the number of Foxa2^{+} and Nkx2.2^{+} cells between *Cdo*^{−/−} and *Shh*^{+/−}*; Cdo*^{−/−} embryos (p = 0.0097 and p = 0.0006, respectively).

only; most remain both Foxa2^{+} and Nkx2.2[+] (Figure 2B). The total number of Foxa2^{+} cells is also reduced (Figure 2C). Coupled with this reduction in Foxa2^{+} cells there is a corresponding decrease in the Shh-producing floor plate (Figure 2B). In *Cdo*^{−/−}*; Shh*^{+/−} mutants, this phenotype is enhanced; in some embryos a few remaining Shh[+], Foxa2^{+} cells are present at the midline and all such cells are also Nkx2.2[+] (Figures 2B and 2C); in others,

Foxa2 is entirely absent and vp3 Nkx2.2[+] progenitors are also reduced (Figure 2C and data not shown). However, vpMN, Olig2^{+} motor neuron progenitors that are positioned more dorsally are unaffected (Figure 2B). The reduction in vp3, Nkx2.2[+] progenitors most likely reflects reduced levels of normal floor plate-derived Shh, because in *Gli2* mutants, FP specification is lost and a reduction in vp3 progenitors is also observed (Ding et al.,
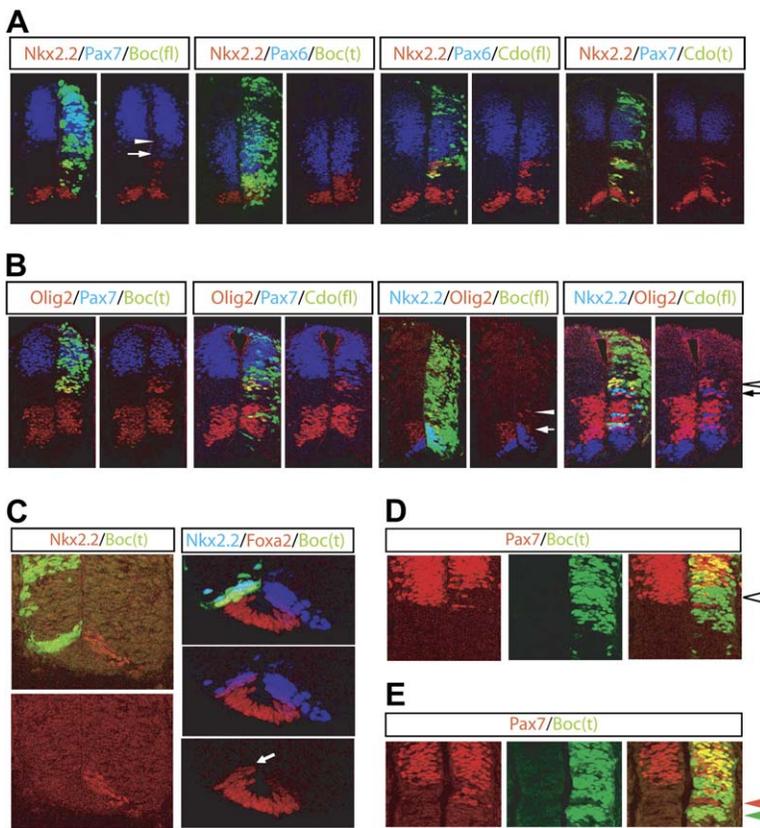
Figure 3. Ectopic Expression of Boc and Cdo Promotes Shh-Dependent Cell Fate Specification in the Shh Target Field

Human *Boc*- or mouse *Cdo*-encoding cDNAs were electroporated unilaterally into the chick neural tube at HH stage 11/12. Neural tube patterning was analyzed at forelimb levels at HH stage 21/22 with cell-type-specific antibody markers. Dorsal is at the top in all panels. Electroporated cells coexpress GFP and are green in all panels.

(A and B) Both full-length (fl) and cytoplasmically truncated (t) forms of *Boc* and *Cdo* activate ectopic Nkx2.2 and Olig2 in more dorsal positions in the Shh target field, repress Pax6 within the Shh target field, and repress both Pax6 and Pax7 (arrowhead in [A]) just dorsal to the D-V intersect. Cell-non-autonomous ventral expansion of Pax7 is also detected (arrow in [A]). When Olig2 and Nkx2.2 are examined in the same section, ectopic Olig2^{+} (arrowhead in [B]) cells lie dorsal to ectopic Nkx2.2[+] (arrow in [B]) progenitors. The lower concentration of Cdo plasmid injected (necessitated by a pronounced growth arrest at higher concentrations) leads to a weaker GFP signal that is somewhat masked in overlays.

(C) *Boc* expression in the Nkx2.2 domain leads to silencing of Nkx2.2 and ectopic Foxa2 (arrowed).

(D) A cell autonomous repression of Pax7 dorsal cell identities (upper open arrowhead).

(E) A cell-non-autonomous ventral expansion of Pax7 ventral cell identities (red arrowhead), following ectopic expression of *Boc* (green arrowhead).

1998). In summary, *Cdo* is essential for normal floor plate specification and interacts with the Shh signaling pathway in this process.

To further address interactions between Boc, Cdo, and the Shh pathway, we ectopically expressed *Boc* and *Cdo* in the neural tube of the developing chick embryo. Shh patterns the presumptive spinal cord by modulating the expression of transcriptional regulators that determine specific neural cell fates (Briscoe and Ericson, 2001; Jessell, 2000). For example, class I genes, such as *Pax6* and *Pax7*, are repressed by Shh signaling, while class II genes, which include *Nkx2.2* and *Olig2*, are activated (Briscoe et al., 2000). Ectopic expression of cDNA constructs encoding either full-length (fl) Cdo or Boc, or truncated forms (t) of both factors that lack the intracellular domain, results in common phenotypes: cell autonomous repression of Pax6 and dorsal expansion of Nkx2.2[+] vp3 progenitors, Olig2^{+} motor neuron progenitors (vpMN), and Foxa2^{+} floor plate (Figures 3A–3C, Figure S3, and data not shown). Importantly, where different ectopic cell identities are observed in the same section, progenitors show a normal, relative distribution. For example, ectopic Olig2^{+} vpMN progenitors always lie dorsal to ectopic Nkx2.2[+] vp3 progenitors (Figure 3B and data not shown).

Pax7 broadly marks dorsal cell identities, the ventral-most of which lie at the normal limit of Shh signaling and overlap the dorsal limits of detectable Shh protein (Gritli-Linde et al., 2001; Wijgerde et al., 2002; C. Chamberlain and A.P.M., unpublished data). Ectopic expression of

Cdo and upregulation of *Boc* in this region (*Boc* is weakly expressed normally; see Figure S2), but not in more dorsal positions, leads to a cell autonomous repression of Pax7 (Figure 3A, far left panel, and Figure 3D). In contrast, when *Boc* or *Cdo* are extensively expressed within the Shh target field just ventral to the normal Pax7 domain, a cell nonautonomous expansion of Pax7^{+} cells is observed into the normal Shh target field (Figure 3A, far left panel, and Figure 3E).

These results lead to several conclusions. First, expression of Boc and Cdo promotes the adoption of more ventral neural identities than is appropriate for cells at a given D-V position. However, the relative position of ectopic cell identities to one another is normal, suggesting that polarity cues are still observed, as expected if Cdo- and Boc-mediated inductions are Shh dependent. Further, while elevated levels of *Cdo* and *Boc* can repress Pax7^{+} fates, repression is only observed close to the D-V boundary, where low levels of Shh are both present and active based on direct analysis of Shh protein distribution and the expression of *Ptch1* and *Gli1*, transcriptional targets of the pathway. In all these instances we only observe a cell autonomous action of Cdo and Boc, consistent with their directly modulating Shh signaling input to the ectopically expressing cells. Second, the cell nonautonomous appearance of more dorsal cell fates above a strong area of *Boc* or *Cdo* expression is suggestive of phenotypes observed when Shh is sequestered by ectopic expression of Hhip1 (Stamataki et al., 2005). This may indicate that either Boc or Cdo

themselves bind Shh, or their activity promotes Shh retention indirectly. Third, both Cdo and Boc appear to have similar properties, as each generates a similar phenotype. Although Cdo and Boc can associate with each other (Kang et al., 2002), this association does not appear to be necessary to promote ventralization. Fourth, in their molecular action, the intracellular domain is dispensable for ventralizing activity, whereas the transmembrane domain is not (data not shown). Together, these data are consistent with a model in which the ectodomains of Cdo and Boc bind to and sequester Shh ligand, thereby enhancing Shh signaling cell autonomously where ligand is available but also potentially limiting Shh movement to more dorsal positions in the normal target field.

To address whether the action of Cdo and Boc are indeed specific for HH signaling, we performed coelectroporation studies with HH pathway-specific components that are known to act at the level of ligand binding and ligand-dependent feedback regulation of membrane signaling. $Ptch1^{\Delta loop2}$ encodes a modified form of the HH-receptor Ptch1 in which removal of one of two extracellular loops prevents ligand binding (Briscoe et al., 2001). As ligand binding to Ptch1 is required to block Ptch1-mediated inhibition of Smo activity, and Smo activity is required for the specification of all HH-dependent cell fates, expression of $Ptch1^{\Delta loop2}$ specifically inhibits ligand-dependent signaling at the level of Ptch1-Smo. As expected if the ectopic induction of ventral cell identities by Cdo and Boc is dependent on Shh ligand-based signaling, coexpression of $Ptch1^{\Delta loop2}$ with Boc results in a cell autonomous inhibition of Boc-mediated ventralization (Figure 4A, lower panel). Importantly, where cells express only Boc, ectopic ventral cell identities are observed (Figure 4A, upper panel). Expression of $Ptch1^{\Delta loop2}$ is associated with ventral cells ectopically activating the dorsal marker Pax7; inhibition of Pax7 is the lowest Shh threshold response reported to date: less than 500 pM of Shh is sufficient in in vitro assays to abolish Pax7 expression, whereas greater than 4 nM is required for floor plate induction (Ericson et al., 1997). As expected, ectopic ventral expression of $Ptch1^{\Delta loop2}$ results in ectopic Pax7+ cells (Figure 4B, upper panel). However, coexpression of Boc suppresses this phenotype (Figure 4B, lower panel). These results suggest that, where ligand is available, Boc enhancement of Shh signaling is sufficient to overcome the inhibitory effects of $Ptch1^{\Delta loop2}$, providing sufficient, minimal level signaling to enable Pax7 repression, but insufficient for ectopic induction of Nkx2.2+ vp3 progenitors. In support of this model, electroporation with a constitutive repressor form of Gli3 (Gli3R) that is insensitive to Shh signaling results in a cell autonomous ventral expansion of Pax7+ cells that cannot be inhibited by coelectroporation with Boc (Figure S4). Hhip1 encodes a second, membrane-associated feedback antagonist that binds ligand directly (Chuang and McMahon, 1999). Hence, ectopic expression of Hhip1 acts to downregulate HH signaling cell autonomously in HH responding cells. We also coexpressed Boc with Hhip1; however, ectopic expression of Hhip1 alone leads to a severe growth defect and an apparent loss of viability in ventral progenitors, precluding further study (data not shown).
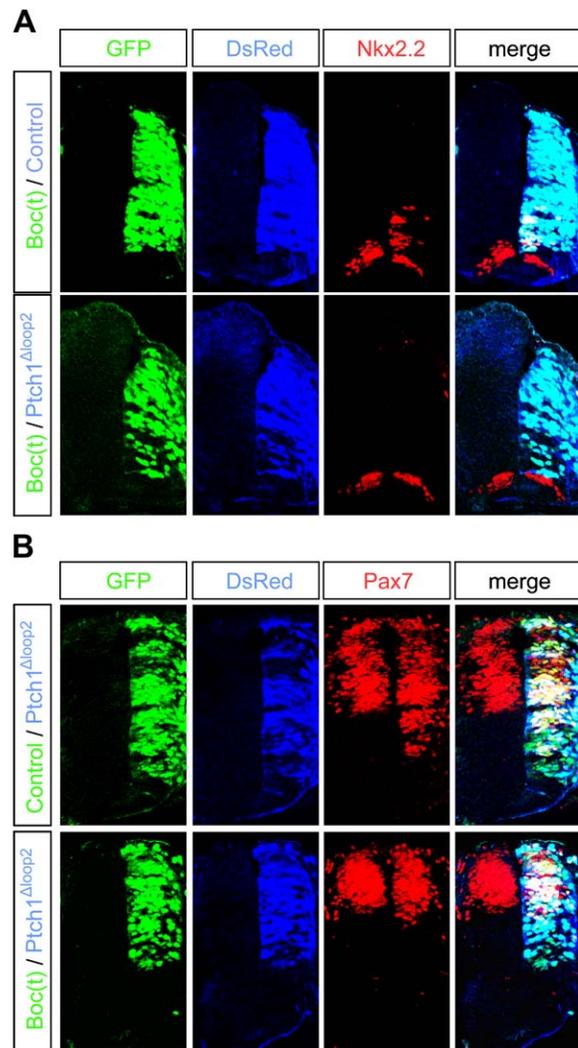

Figure 4. Coexpression of *Boc* with $Ptch1^{\Delta loop2}$ Abrogates the Effects of Boc-Mediated Enhancement of Ventral Cell Fate Specification

Plasmid constructs encoding cytoplasmically truncated Boc(t) (GFP coexpression) or Ptch1$^{\Delta loop2}$ (DsRed coexpression) were electroporated into the chick neural tube, and the expression of (A) vp3 (Nkx2.2+) and (B) dorsal (Pax7+) progenitors was assayed by immunohistochemistry as indicated. Control DNAs consist of base vectors producing only GFP or DsRed.

Cdo and Boc Bind Shh Directly through a Specific Fibronectin Repeat

The data above are most readily explained if Cdo and Boc play a direct role in Shh signaling, rather than indirectly modifying signaling by other factors such as members of the Tgf-β superfamily that play opposite roles to Shh in patterning the dorsal neural tube. Together, the Shh ligand-dependent action of Cdo and Boc and their cell surface localization suggest that they could act through binding of Shh ligand. To address this possibility, we examined binding of a secreted form of an N-Shh::AP fusion protein (the N-terminal signaling moiety of Shh fused at its C terminus to alkaline phosphatase [AP]) to Cos7 cells expressing Hhip1 (positive control), *Boc*, *Cdo*, and as a negative control, *Frizzled-3* (*Fz3*), a putative Wnt receptor (Figures 5A and 5B). Only cells
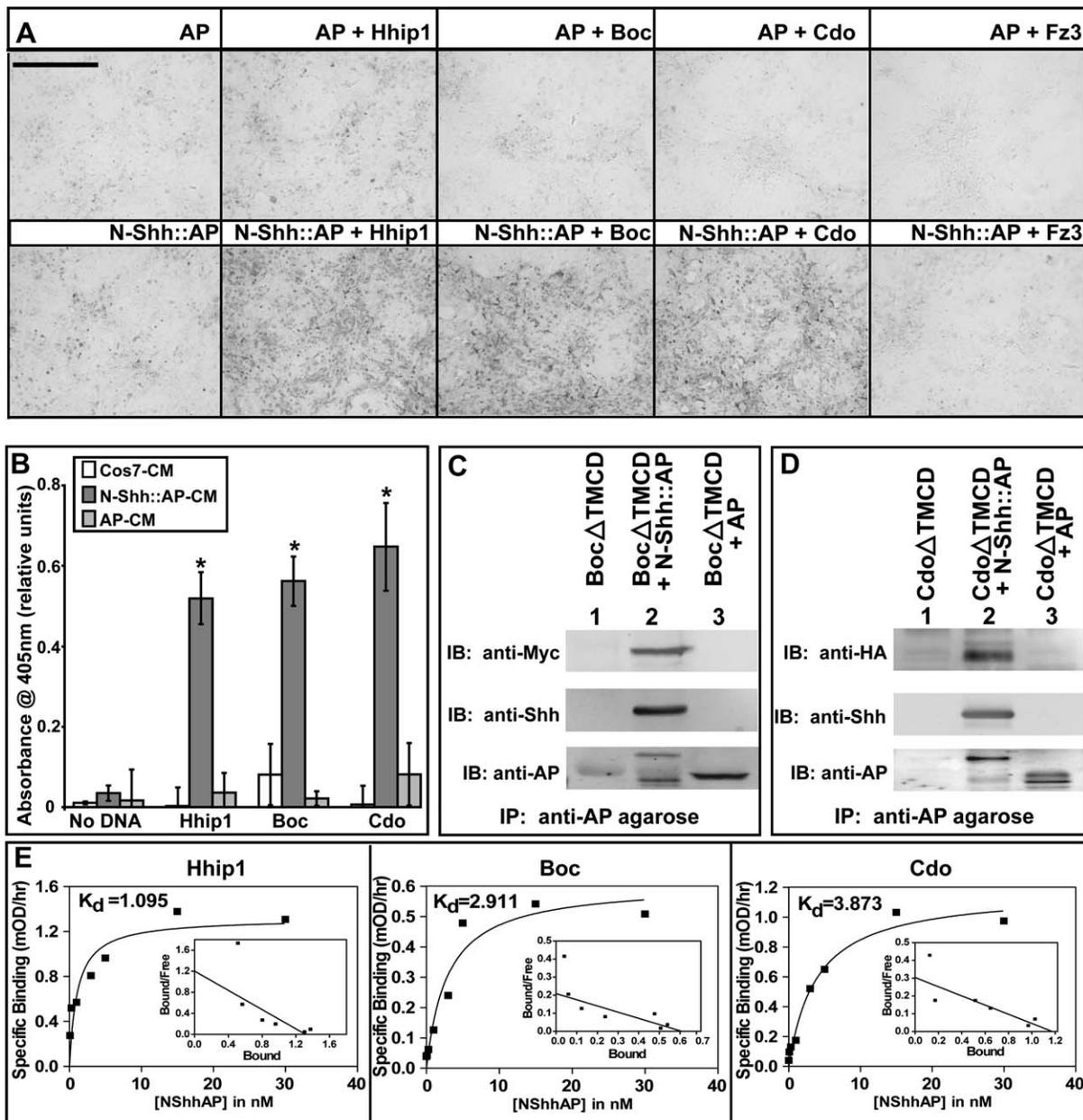
Figure 5. Cdo and Boc Bind Shh

(A) Binding of N-Shh::AP to *Cdo*- and *Boc*-expressing cells. Scale bar, 50 μm.

(B) Quantitation of N-Shh::AP binding to Cdo and Boc. Error bars represent the mean ± SD of four identical treatment groups. Significant differences between binding of N-Shh::AP and AP conditioned medium (CM) are indicated by * (two-tailed student t test, $p < 0.01$).

(C and D) (C) Immunoprecipitation of Boc and (D) immunoprecipitation of Cdo extracellular domains (BocΔTMCD and CdoΔTMCD, respectively) with Shh. Cos7 cells were transfected with BocΔTMCD or CdoΔTMCD alone (lane 1), or cotransfected with N-Shh::AP (lane 2) or AP (lane 3). Complexes were immunoprecipitated from supernatants with anti-AP beads. Epitope-labeled BocΔTMCD was detected following Western blot analysis of immunoprecipates with anti-Myc antibody, and epitope-tagged CdoΔTMCD with anti-HA antibody. N-Shh::AP was detected with anti-Shh antibody or anti-AP; the latter was also used to detect AP.

(E) Dissociation constant (K_d) measurements. Saturation binding curves and Scatchard analysis (insets) of NShh::AP binding to Hhip1 (left), Boc (middle), and Cdo (right). Each point on the graphs represents the average of three identical treatment groups.

expressing *Hhip1*, *Boc*, and *Cdo* bind N-Shh::AP, binding is Shh-dependent (i.e., AP alone does not bind), and both Boc and Cdo bind N-Shh::AP as effectively as Hhip1 (Chuang and McMahon, 1999). We next examined whether binding represents a direct association of Shh with either Boc or Cdo. When N-Shh::AP and epitope-tagged, secreted forms of Boc or Cdo (BocΔTMCD and CdoΔTMCD) are cotransfected into Cos7 cells and supernatants are assayed, we detect N-Shh::AP/BocΔTMCD and N-Shh::AP/CdoΔTMCD complexes, indicating that Shh binds to both Boc and Cdo ectodomains (Figures 5C and 5D). The use of secreted forms reduces the possibility that unknown, cell surface bound factors promote binding or contribute directly to the complex.
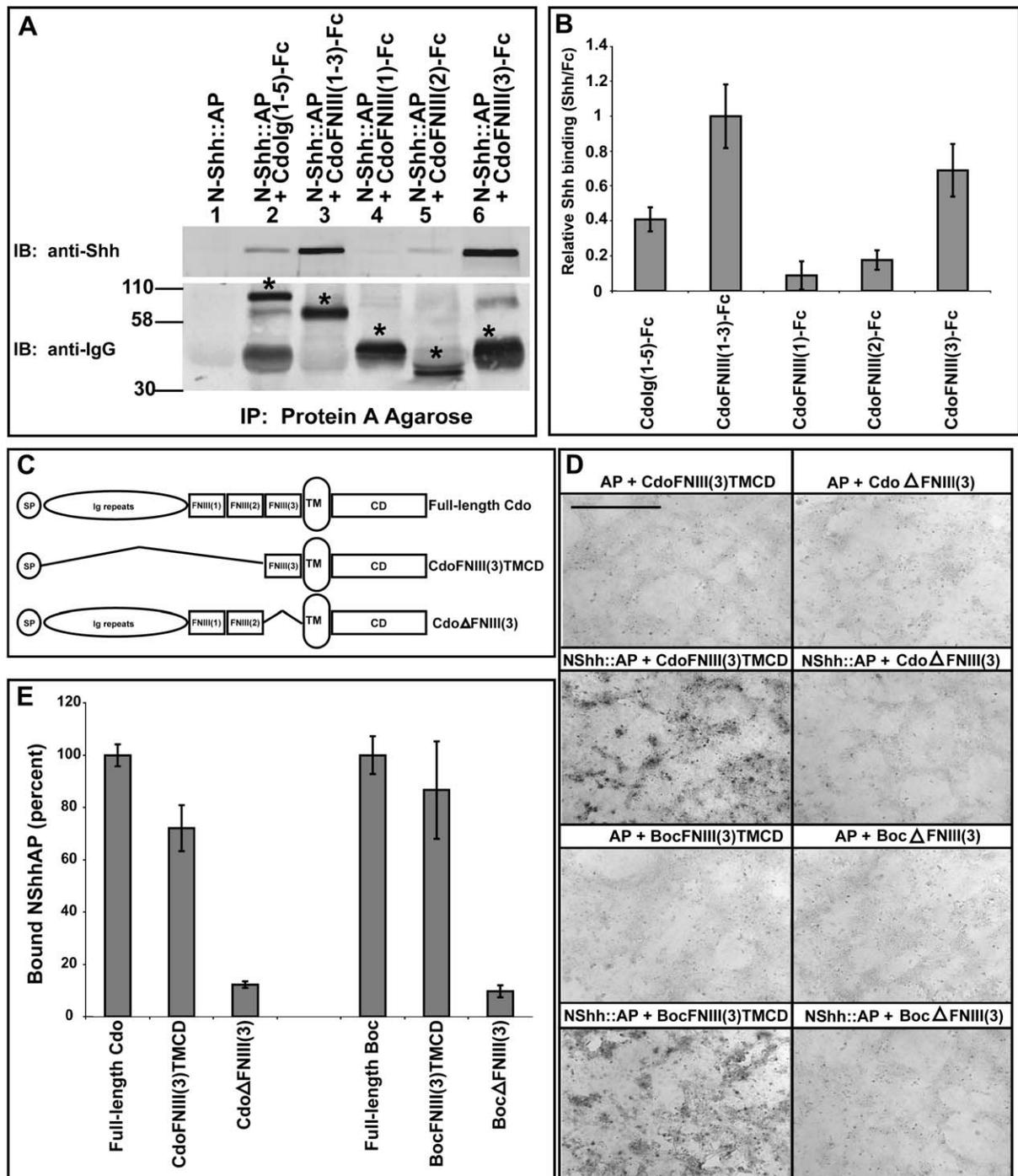
Figure 6. Mapping of Shh Binding Domains in Cdo and Boc

(A) Cos7 cells transfected with N-Shh::AP alone (lane 1) or cotransfected with various Cdo ectodomain Fc fusion constructs (lanes 2–6). Complexes were immunoprecipitated from conditioned medium with Protein A agarose. Top panel: Detection of N-Shh::AP with anti-Shh. Bottom panel: Identification of Fc fusion proteins with anti-human IgG. Asterisks highlight the various Fc fusion proteins as confirmed by comparison with the migration of molecular weight markers (left).

(B) Quantitation of relative Shh binding to each Cdo-Fc fusion proteins. Binding is expressed as a ratio of Shh band intensity/Cdo-Fc band intensity.

(C) Schematic of Cdo mutant constructs. Full-length Cdo (top) is contrasted with constructs expressing only the FNIII(3) domain of the Cdo [CdoFNIII(3)TMCD, middle] or constructs that express the entire extracellular domain except for the FNIII(3) domain [CdoΔFNIII(3), bottom]. Identical constructs were also generated for Boc.

(D) Binding of NShh::AP to Cdo and Boc constructs containing the third FNIII repeat [CdoFNIII(3)TMCD and BocFNIII(3)TMCD, respectively] or lacking the third FNIII repeat [CdoΔFNIII(3) and BocΔFNIII(3), respectively]. Scale bar, 50 μm.

(E) Quantitation of N-Shh::AP binding to full-length and truncated Cdo and Boc constructs.

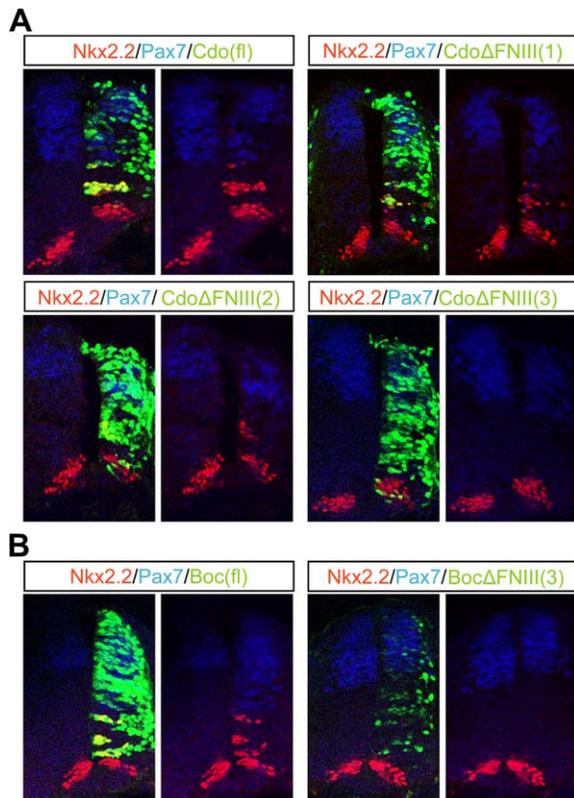Error bars represent the mean ± SD of four identical treatment groups.

Figure 7. The FNIII(3) Domains in Both Cdo and Boc Are Necessary for Enhancement of Shh Signaling in the Developing Chick Neural Tube

(A) Expression of Nkx2.2[+] (red) or Pax7^{+} (blue) neural cell progenitors in chick neural tubes electroporated with full-length Cdo (top left panels), CdoΔFNIII(1) (top right panels), CdoΔFNIII(2) (bottom left panels), or CdoΔFNIII(3) (bottom right panels). Green cells indicate GFP expression in electroporated cells.

(B) Expression of neural cell progenitor markers in chick neural tubes following electroporation with full-length Boc (left panels) or BocΔFNIII(3) (right panels).

To determine the affinity of the Shh-Boc and Shh-Cdo interactions, saturation binding experiments were performed using Cos7 cells transfected with *Boc*, *Cdo*, or *Hhip1* for comparison (Figure 5E). Calculation of the dissociation constants (K_d) for NShh::AP binding to Boc and Cdo yielded similarly high affinities (approximately 3 and 4 nM, respectively), while a K_d of 1 nM for Hhip1 is in close agreement with previously published data (Chuang and McMahon, 1999).

Having established that Boc and Cdo interact with Shh with high affinity, we performed domain-mapping analysis to define the region of Boc and Cdo that binds to Shh (Figure 6). Immunoprecipitation experiments using Fc-fusion constructs that contain either the Ig-like domains or FNIII domains of Cdo indicate that the fibronectin repeat-containing region plays the major role in Shh binding (Figure 6A). Furthermore, analysis of constructs expressing each FNIII domain singly suggests that most binding can be ascribed to the FNIII(3) domain, the most highly conserved of these repeats (Figures 6A and 6B). To further confirm the importance of this domain in Cdo and Boc, NShh::AP binding assays

were performed using constructs whose extracellular domains consist of only the third FNIII repeat (CdoFNIII(3)TMCD and BocFNIII(3)TMCD) or the entire extracellular domain except for the third FNIII repeat (CdoΔFNIII(3) and BocΔFNIII(3), Figures 6C–6E). In these assays, the FNIII(3) domain of Cdo and Boc is both necessary and sufficient to specifically mediate NShh::AP binding to Cos7 cells, indicating that this region plays a critical role in these interactions.

Cdo and Boc Binding to Shh Is Necessary, but Not Sufficient, to Ectopically Activate Shh Signaling

To test whether the FNIII(3) domains of Cdo and Boc are necessary to augment Shh signaling, chick electroporation experiments were performed with a series of Cdo and Boc constructs (Figure 7 and Figure S5). Expression of full-length Cdo or Boc results in ectopic activation of Nkx2.2 (Figure 7A, top left panels, and Figure 7B, left panels, respectively), as does expression of Cdo constructs lacking either FNIII(1) (Figure 7A, top right panels) or FNIII(2) (Figure 7A, bottom left panels). In contrast, Cdo or Boc lacking FNIII(3) fails to ectopically activate Nkx2.2, despite strong ventral expression of these variants (Figure 7A, bottom right panel, and Figure 7B, right panels, respectively). Despite the clear requirement for FNIII(3) in Shh binding and activity, the FNIII(3) domain alone of either Boc or Cdo is not sufficient to reproduce Cdo- or Boc-dependent phenotypes within the neural tube (Figure S5). Thus, Cdo and Boc most likely promote signaling by binding Shh in conjunction with interactions requiring other regions of their extracellular domains. Understanding these interactions may provide some insight into why some Shh binding proteins, such as Boc and Cdo, function as positive regulators of Shh signaling, while others, such as Hip1, function as negative regulators. These studies, together with those in the accompanying paper (Zhang et al., 2006), identify Boc and Cdo as novel components of the vertebrate Hedgehog signaling pathway. A report that a related gene is required for normal HH signaling in *Drosophila* tissue culture cells suggests this function is conserved (Lum et al., 2003). Considering all the genetic, biochemical, and expression analyses, we propose a model wherein Cdo and Boc enhance HH signaling at two critical positions within a postulated HH activity gradient: (1) where the highest signaling levels are required in FP specification and (2) at the fringes of a HH target field, close to the D-V intersect in the neural tube and possibly also at the anterior limit of signaling in the limb bud. At these latter positions, where ligand levels are expected to be low, this mechanism may increase the robustness of signaling. Additionally, the negative regulation of Boc and Cdo expression by HH signaling would restrict Cdo/Boc-mediated enhancement of HH signaling to the relevant region, establishing by this feedback system an appropriate domain for their action. While the current model is clearly speculative, the future analysis of *Boc* mutants and *Cdo; Boc* compound mutants, along with further biochemical and cellular analyses, should provide important tests of these ideas.

Our data provide two critical mechanistic insights; first, Cdo and Boc both bind Shh via their FNIII(3) domains, and second, Cdo and Boc binding to Shh is necessary for enhancement of Shh signaling. We suggest

that Shh/Cdo or Shh/Boc complexes either facilitate presentation of active ligand to Ptch1, or that binding counteracts feedback-mediated sequestration of ligand and ligand turnover, increasing effective levels of signaling in a responding cell. Thus, Cdo and Boc appear to represent a new class of factors in the increasingly complex Shh feedback network; expression of each is broadly negatively regulated by HH signaling, but their activity stimulates HH signaling. Importantly, the accompanying work of Zhang et al. (2006) identifies Cdo as a modulator of Shh signaling in holoprosencephaly, implicating these genes as potential interacting factors in Shh-related human pathologies.

Experimental Procedures

Transcriptional Profiling
The transcriptional profiling will be described in detail elsewhere (TT and APM, in preparation). Briefly, RNA was prepared from 6–8 and 10–13 somite stage wild-type, $Ptch1^{-/-}$ (Goodrich et al., 1997) and $Smo^{-/-}$ (Zhang et al., 2001) embryos, and from head and limb buds isolated from E10.5 wild-type and $Shh^{-/-}$ (St-Jacques et al., 1998) embryos. RNAs were used in standard procedures to generate probes for analysis of transcript expression on Affymetrix U74Av2 and M430 A and B microarrays. Data were statistically analyzed using Resolver software (Rosetta).

Mice
Mouse experiments were carried out largely on a 129 background as in the original Cdo report; hence the "weak" midline defects in the $Cdo^{-/-}$ embryos in this study. The Shh mutant allele on a 129/Sv; C57BL6/J; CBA/J hybrid background was crossed with $Cdo^{+/-}$ stock (129/Sv; C57BL6) and the phenotypes of littermates examined in this mixed background ($Cdo^{-/-}$, n = 14; $Cdo^{-/-}$; $Shh^{+/-}$, n = 13). The strongest midline defects in Cdo$^{-/-}$ littermates were always observed in those carrying the Shh null allele.

Generation of Cdo and Boc Constructs
All constructs were generated using standard molecular biology procedures (Maniatis et al., 1982). Briefly, cytoplasmic truncations of Boc and Cdo [Boc(t) and Cdo(t)] deleted aa 79–1115 of human Boc and aa 986–1251 of mouse Cdo. Soluble versions of Boc and Cdo that lack both the transmembrane and cytoplasmic domains (BocΔTMCD and CdoΔTMCD) were truncated at aa 855 and aa 958 of Boc and Cdo, respectively. Constructs encoding the third FNIII repeat, transmembrane, and cytoplasmic domains of Boc [BocFNIII(3)TMCD] and Cdo [CdoFNIII(3)TMCD] were fused to their respective signal peptides at aa 712 of Boc and aa 830 of Cdo. Constructs encoding Boc and Cdo that lack the third FNIII repeat [BocΔFNIII(3) and CdoΔFNIII(3), respectively] deleted aa 710–809 of Boc and aa 832–919 of Cdo. All constructs were cloned into pCIG.

Cdo-Fc fusion proteins were generated by PCR amplification of each of the indicated regions as follows: CdoIg(1–5)-Fc (aa 1–575), CdoFNIII(1–3)-Fc (aa 534–959), CdoFNIII(1)-Fc (aa 534–711), CdoFNIII(2)-Fc (aa 662–814), and CdoFNIII(3)-Fc (aa 802–959). The FNIII constructs were then fused in-frame to native mouse Cdo start codon and signal sequence (aa 1–41), followed by the cloning of all constructs into the Igtag vector (Bergemann et al., 1995).

AP Binding Assays
These experiments were performed essentially as described previously (Flanagan et al., 2000). Briefly, Cos-7 cells were transfected with either AP or N-Shh::AP alone, or cotransfected with full-length mouse Hhip1 (Chuang and McMahon, 1999), mouse Cdo (Kang et al., 1997), human Boc (Kang et al., 2002), or mouse Fz3. Bound AP protein was visualized with BM purple AP substrate (Roche) for cell surface staining, or with AP yellow liquid substrate (Sigma) to quantify AP binding in cell extracts. Saturation binding curves and Scatchard analysis were performed using GraphPad Prism version 4.03 for Windows (GraphPad Software, San Diego, CA). K_d measurements were determined by nonlinear regression analysis of the saturation binding data.

Immunoprecipitation Analysis
Cos-7 cells were transfected using Lipofectamine 2000 (Invitrogen), and conditioned medium was collected 48 hr after transfection. Immunoprecipitation of AP and N-Shh::AP from conditioned medium was performed by incubation with anti-AP agarose beads (Sigma) overnight at 4°C on a rotator. Beads were washed three times with buffer (50 mM Tris [pH 7.6], 500 mM NaCl, 1% TritonX-100), resuspended in Laemmli sample buffer, heated at 95°C for 5 min, and analyzed by SDS-PAGE and Western blot analysis. AP and N-Shh::AP were detected with rabbit anti-AP antibody (Biomeda). Myc epitope-tagged BocΔTMCD was detected with mouse anti-myc antibody (clone 9E10; Developmental Studies Hybridoma Bank). HA-tagged CdoΔTMCD was identified with mouse anti-HA antibody (Covance). Rabbit anti-Shh antibody has been described previously (Bumcrot et al., 1995).

In Situ Hybridization and Immunofluorescence
Whole-mount digoxigenin in situ hybridization was performed as described on wild-type and mutant embryos (Wilkinson, 1992). Section in situ hybridization was carried out on 30 μm sections with digoxigenin probes at forelimb-levels. Immunofluorescence analysis was performed on 10 μm frozen sections; image collection was carried out on a Zeiss LSM510 confocal microscope. The following antibodies were used: rabbit anti-Olig2 (1:5000), mouse anti-Foxa2 (1:5), rabbit anti-Nkx2.2 (1:4000), mouse anti-Pax7 (1:20), mouse anti-Pax6 (1:20), rabbit anti-Olig2 (1:5000), mouse anti-Shh (1:25, Developmental Studies Hybridoma Bank), Alexa 568 or 633 goat anti-rabbit or goat anti-mouse (1:300, Molecular Probes) and rabbit anti-DsRed (1:400, BD Bioscience).

Chick Electroporation
Boc or Cdo and their derivatives and Gli3R (a gift of S. Vokes) were cloned into pCIG vector (Megason and McMahon, 2002) to enable coexpression of Boc and Cdo with GFP to visualize electroporated cells. $Ptch1^{\Delta loop2}$ (Briscoe et al., 2001) was cloned into pCIR. In this vector, the GFP-encoding cDNA of pCIG was replaced by one encoding Red fluorescent protein (DsRed-Express, Invitrogen). For electroporation, Qiagen-purified, supercoiled plasmid DNA was injected into the neural tubes of Hamburger-Hamilton (HH) stage 11–12 chicken embryos (Hamburger and Hamilton, 1992). Boc and Cdo were injected at concentrations of 1.0 or 0.7 μg/μl in PBS, respectively, with 50 ng/μl Fast Green. In coelectroporation studies, both DNAs were at a concentration of 1.5 μg/μl. Electrodes were made from 0.5 mm diameter platinum wire (Aldrich) and were 5 mm long and spaced 5 mm apart. Electrodes were placed flanking the neural tube, covered with a drop of PBS, and pulsed five times at 25 V for 50 ms with a BTX Electroporator (Genetronics). Embryos were recovered after 48 hr at HH stage 21–22 and fixed for immunohistochemistry. Each analysis was repeated a minimum of 20 times.

Supplemental Data
Supplemental Data including five figures are available at http://www.developmentalcell.com/cgi/content/full/10/5/647/DC1/.

References

Bergemann, A.D., Cheng, H.J., Brambilla, R., Klein, R., and Flanagan, J.G. (1995). ELF-2, a new member of the Eph ligand family, is segmentally expressed in mouse embryos in the region of the hindbrain and newly forming somites. Mol. Cell. Biol. *15*, 4921–4929.

Briscoe, J., and Ericson, J. (2001). Specification of neuronal fates in the ventral neural tube. Curr. Opin. Neurobiol. *11*, 43–49.

Briscoe, J., Pierani, A., Jessell, T.M., and Ericson, J. (2000). A homeodomain protein code specifies progenitor cell identity and neuronal fate in the ventral neural tube. Cell *101*, 435–445.

Briscoe, J., Chen, Y., Jessell, T.M., and Struhl, G. (2001). A hedgehog-insensitive form of patched provides evidence for direct long-range morphogen activity of sonic hedgehog in the neural tube. Mol. Cell *7*, 1279–1291.

Bumcrot, D.A., Takada, R., and McMahon, A.P. (1995). Proteolytic processing yields two secreted forms of sonic hedgehog. Mol. Cell. Biol. *15*, 2294–2303.

Chiang, C., Litingtung, Y., Lee, E., Young, K.E., Corden, J.L., Westphal, H., and Beachy, P.A. (1996). Cyclopia and defective axial patterning in mice lacking Sonic hedgehog gene function. Nature *383*, 407–413.

Chuang, P.T., and McMahon, A.P. (1999). Vertebrate Hedgehog signalling modulated by induction of a Hedgehog-binding protein. Nature *397*, 617–621.

Cole, F., and Krauss, R.S. (2003). Microform holoprosencephaly in mice that lack the Ig superfamily member Cdon. Curr. Biol. *13*, 411–415.

Cooper, M.K., Porter, J.A., Young, K.E., and Beachy, P.A. (1998). Teratogen-mediated inhibition of target tissue response to Shh signaling. Science *280*, 1603–1607.

Ding, Q., Motoyama, J., Gasca, S., Mo, R., Sasaki, H., Rossant, J., and Hui, C.C. (1998). Diminished Sonic hedgehog signaling and lack of floor plate differentiation in Gli2 mutant mice. Development *125*, 2533–2543.

Echelard, Y., Epstein, D.J., St-Jacques, B., Shen, L., Mohler, J., McMahon, J.A., and McMahon, A.P. (1993). Sonic hedgehog, a member of a family of putative signaling molecules, is implicated in the regulation of CNS polarity. Cell *75*, 1417–1430.

Ericson, J., Rashbass, P., Schedl, A., Brenner-Morton, S., Kawakami, A., van Heyningen, V., Jessell, T.M., and Briscoe, J. (1997). Pax6 controls progenitor cell identity and neuronal fate in response to graded Shh signaling. Cell *90*, 169–180.

Flanagan, J.G., Cheng, H.J., Feldheim, D.A., Hattori, M., Lu, Q., and Vanderhaeghen, P. (2000). Alkaline phosphatase fusions of ligands or receptors as in situ probes for staining of cells, tissues, and embryos. Methods Enzymol. *327*, 19–35.

Goodrich, L.V., Milenkovic, L., Higgins, K.M., and Scott, M.P. (1997). Altered neural cell fates and medulloblastoma in mouse patched mutants. Science *277*, 1109–1113.

Gritli-Linde, A., Lewis, P., McMahon, A.P., and Linde, A. (2001). The whereabouts of a morphogen: direct evidence for short- and graded long-range activity of hedgehog signaling peptides. Dev. Biol. *236*, 364–386.

Gritli-Linde, A., Bei, M., Maas, R., Zhang, X.M., Linde, A., and McMahon, A.P. (2002). Shh signaling within the dental epithelium is necessary for cell proliferation, growth and polarization. Development *129*, 5323–5337.

Hamburger, V., and Hamilton, H.L. (1992). A series of normal stages in the development of the chick embryo. 1951. Dev. Dyn. *195*, 231–272.

Ingham, P.W., and McMahon, A.P. (2001). Hedgehog signaling in animal development: paradigms and principles. Genes Dev. *15*, 3059–3087.

Jeong, Y., and Epstein, D.J. (2003). Distinct regulators of Shh transcription in the floor plate and notochord indicate separate origins for these tissues in the mouse node. Development *130*, 3891–3902.

Jeong, J., and McMahon, A.P. (2005). Growth and pattern of the mammalian neural tube are governed by partially overlapping feedback activities of the hedgehog antagonists patched 1 and Hhip1. Development *132*, 143–154.

Jeong, J., Mao, J., Tenzen, T., Kottmann, A.H., and McMahon, A.P. (2004). Hedgehog signaling in the neural crest cells regulates the patterning and growth of facial primordia. Genes Dev. *18*, 937–951.

Jessell, T.M. (2000). Neuronal specification in the spinal cord: inductive signals and transcriptional codes. Nat. Rev. Genet. *1*, 20–29.

Kang, J.S., Gao, M., Feinleib, J.L., Cotter, P.D., Guadagno, S.N., and Krauss, R.S. (1997). CDO: an oncogene-, serum-, and anchorage-regulated member of the Ig/fibronectin type III repeat family. J. Cell Biol. *138*, 203–213.

Kang, J.S., Mulieri, P.J., Hu, Y., Taliana, L., and Krauss, R.S. (2002). BOC, an Ig superfamily member, associates with CDO to positively regulate myogenic differentiation. EMBO J. *21*, 114–124.

Lee, C.S., Buttitta, L., and Fan, C.M. (2001). Evidence that the WNT-inducible growth arrest-specific gene 1 encodes an antagonist of sonic hedgehog signaling in the somite. Proc. Natl. Acad. Sci. USA *98*, 11347–11352.

Lum, L., Yao, S., Mozer, B., Rovescalli, A., Von Kessler, D., Nirenberg, M., and Beachy, P.A. (2003). Identification of Hedgehog pathway components by RNAi in *Drosophila* cultured cells. Science *299*, 2039–2045.

Maniatis, T., Fritsch, E.F., and Sambrook, J. (1982). Molecular Cloning: A Laboratory Manual (Cold Spring Harbor, NY: Cold Spring Harbor Laboratory).

McMahon, A.P., Ingham, P.W., and Tabin, C.J. (2003). Developmental roles and clinical significance of hedgehog signaling. Curr. Top. Dev. Biol. *53*, 1–114.

Megason, S.G., and McMahon, A.P. (2002). A mitogen gradient of dorsal midline Wnts organizes growth in the CNS. Development *129*, 2087–2098.

Mulieri, P.J., Okada, A., Sassoon, D.A., McConnell, S.K., and Krauss, R.S. (2000). Developmental expression pattern of the cdo gene. Dev. Dyn. *219*, 40–49.

Mulieri, P.J., Kang, J.S., Sassoon, D.A., and Krauss, R.S. (2002). Expression of the boc gene during murine embryogenesis. Dev. Dyn. *223*, 379–388.

St-Jacques, B., Dassule, H.R., Karavanova, I., Botchkarev, V.A., Li, J., Danielian, P.S., McMahon, J.A., Lewis, P.M., Paus, R., and McMahon, A.P. (1998). Sonic hedgehog signaling is essential for hair development. Curr. Biol. *8*, 1058–1068.

Stamataki, D., Ulloa, F., Tsoni, S.V., Mynett, A., and Briscoe, J. (2005). A gradient of Gli activity mediates graded Sonic Hedgehog signaling in the neural tube. Genes Dev. *19*, 626–641.

Tian, H., Jeong, J., Harfe, B.D., Tabin, C.J., and McMahon, A.P. (2005). Mouse Disp1 is required in sonic hedgehog-expressing cells for paracrine activity of the cholesterol-modified ligand. Development *132*, 133–142.

Wijgerde, M., McMahon, J.A., Rule, M., and McMahon, A.P. (2002). A direct requirement for Hedgehog signaling for normal specification of all ventral progenitor domains in the presumptive mammalian spinal cord. Genes Dev. *16*, 2849–2864.

Wilkinson, D.G. (1992). In Situ Hybridization: A Practical Approach (Oxford, New York: IRL Press at Oxford University Press).

Zhang, X.M., Ramalho-Santos, M., and McMahon, A.P. (2001). Smoothened mutants reveal redundant roles for Shh and Ihh signaling including regulation of L/R symmetry by the mouse node. Cell *106*, 781–792.

Zhang, W., Kang, J.-S., Cole, F., Yi, M.-J., and Krauss, R.S. (2006). Cdo functions at multiple points in the Sonic Hedgehog pathway and Cdo-deficient mice accurately model human holoprosencephaly. Dev. Cell *10*, this issue, 657–665.